The physical process analysis of the capacitance–voltage characteristics of AlGaN/AlN/GaN high electron mobility transistors*

Wang Xin-Hua(王鑫华), Zhao Miao(赵 妙), Liu Xin-Yu(刘新宇)†,
Pu Yan(蒲 颜), Zheng Ying-Kui(郑英奎), and Wei Ke(魏 珂)

Key Laboratory of Microelectronics Device & Integrated Technology, Institute of Microelectronics of Chinese Academy of Sciences, Beijing 100029, *China*

(Received 3 November 2009; revised manuscript received 24 March 2010)

This paper deduces the expression of the Schottky contact capacitance of AlGaN/AlN/GaN high electron mobility transistors (HEMTs), which will help to understand the electron depleting process. Some material parameters related with capacitance–voltage profiling are given in the expression. Detailed analysis of the forward-biased capacitance has been carried on. The gate capacitance of undoped AlGaN/AlN/GaN HEMT will fall under forward bias. If a rising profile is obviously observed, the donor-like impurity or trap is possibly introduced in the barrier.

Keywords: AlGaN/AlN/GaN, HEMT, capacitance–voltage characteristics, trap
PACC: 7320D, 7280E, 7360L

1. Introduction

High electron mobility transistor (HEMT) with AlGaN/AlN/GaN heterostructures has been adopted recently due to its high two-dimensional electron gas (2DEG) density.[1−3] Many technologies are applied on the analysis of these new heterostructures. The capacitance–voltage (C–V) technology is a well-developed tool for investigating the carrier distribution in the material. The sheet carrier concentration of 2DEG can be deduced from the CV profiling.[4−6] The related trap information in the material can be obtained from the varied frequency CV profiling.[5−8] An appropriate fit of CV profiling will help to analyse the influence on CV profiling with varied factors.[9−11] The potential problem can be fed back to improve the related arts.

The calculations of gate capacitance of GaAs HEMT have been developed in Ref. [12]. We try to deduce the expression of Schottky contact capacitance of the AlGaN/AlN/GaN HEMT based on their method, and investigate the physical process of CV profiling formation in this paper. Combined with the capacitance expression, the physical process of the CV profiling formation is analysed, especially the forward-biased CV profiling. The CV profiling reflects the dynamic process of the depletion region in epilayer. From CV profiling, we can estimate the potential problem in each layer, which will help to generally understand the material and electric characteristics of HEMT.

2. Calculation of the gate capacitance for AlGaN/AlN/GaN HEMTs

Figure 1 is the schematic diagram of the structure and charge distribution of AlGaN/AlN/GaN epilayers, where $\sigma_{\rm AlN}$ and $\sigma_{\rm AlGaN}$ are the densities of the polarisation induced charge at AlN/GaN interface and AlGaN surface, respectively, $\sigma_{\rm surface}$ is the charge density at AlGaN surface, $\sigma_{\rm 2DEG}$ is the charge density of 2DEG, $\sigma_{\rm substrate}$ is the charge density in the substrate.

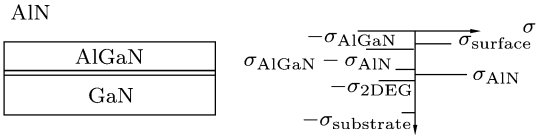


Fig. 1. Schematic diagram of the structure and charge distribution of AlGaN/AlN/GaN epilayers.

According to the electrostatic neutrality:[13]

*Project supported by the National Basic Research Program (973) of China (Grant No. 2010CB327500) and the National Natural Science Foundation of China (Grant Nos. 60976059 and 60890191).
†Corresponding author. E-mail: xyliu@ime.ac.cn
© 2010 Chinese Physical Society and IOP Publishing Ltd

$$\sigma_{\rm surface} - \sigma_{\rm AlGaN} + \sigma_{\rm AlGaN} + \sigma_{\rm AlN} - \sigma_{\rm AlN} - \sigma_{\rm 2DEG} - \sigma_{\rm substrate} = 0,$$

which reduces to

$$\sigma_{\rm surface} = \sigma_{\rm 2DEG} + \sigma_{\rm substrate}. \tag{1}$$

The charge at the metal–semiconductor (M–S) interface can be expressed as follows: $Q_{\rm s} = \sigma_{\rm surface} = qn_{\rm s} + \sigma_{\rm substrate}$, where $n_{\rm s}$ is the sheet carrier density of 2DEG.

So the capacitance per unit area between the gate and source is given by

$$C_{\rm s} = \frac{{\rm d}Q_{\rm s}}{{\rm d}V_{\rm g}} = q\frac{{\rm d}n_{\rm s}}{{\rm d}V_{\rm g}} + \frac{{\rm d}\sigma_{\rm substrate}}{{\rm d}V_{\rm g}}. \tag{2}$$

If the impurity charge density in the substrate is not the function of the gate voltage ($V_{\rm g}$), or there is no impurity charge in the substrate, Eq. (2) reduced to

$$C_{\rm s} = \frac{{\rm d}Q_{\rm s}}{{\rm d}V_{\rm g}} = q\frac{{\rm d}n_{\rm s}}{{\rm d}V_{\rm g}}. \tag{3}$$

The two main sources of 2DEG in GaN HEMT with AlN interlayer are as follows: (1) donors from the doped AlGaN layer; (2) polarisation induced charge. Now the unintentional doped AlGaN structures are widely adopted in the lab, thus, 2DEG almost comes from the polarisation induced charge. Although the resident electron in AlGaN layer is few in comparison with the polarisation induced charge, it is necessary to take the resident electron into consideration during the solution, in order to find out the detailed relation between them.

Figure 2 is the energy band of AlGaN/AlN/GaN HEMT. The basic physical parameters in Fig. 2 are as follows: Schottky barrier height ($\phi_{\rm M}$), gate voltage ($V_{\rm g}$), electric quantity (q), conduction band ($E_{\rm c}$), valence band ($E_{\rm v}$), conduction band-edge discontinuity between AlN and GaN ($q\Delta E_{\rm c1}$), conduction band-edge discontinuity between AlN and AlGaN ($q\Delta E_{\rm c2}$), the Fermi level height above GaN conduction band-edge at the heterointerface ($qE_{\rm F}$), the Fermi level ($qE_{\rm F0}$), the thickness of AlN and AlGaN (d_1, d_2, respectively). We set the interface between AlGaN and AlN as origin and set the subscript (1, 2 and 3) to mark materials (AlN, AlGaN and GaN) for convenience.

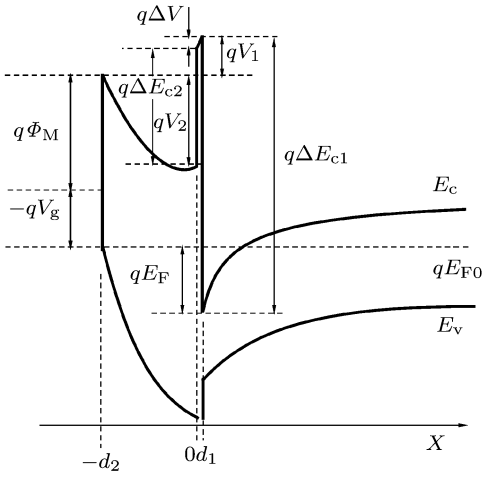


Fig. 2. Energy band of AlGaN/AlN/GaN HEMT.

At $x = d_1$, the Gauss law leads to the following equality:

$$\varepsilon_3 E_{\rm i3} = qn_{\rm s} - qN_{\rm b}W, \tag{4}$$

where ε_3 is the dielectric constant of GaN, $E_{\rm i3}$ is the electric field at heterointerface in the GaN side, $N_{\rm b}$ is ionised resident electron concentration in GaN material, and W is the width of the depletion layer for resident electron.

If we just consider the influence of resident electron ($N_{\rm B}$) in AlGaN on 2DEG, we can obtain the relation between $n_{\rm s}$ and $N_{\rm B}$. We begin to calculate $n_{\rm s}$ following Delagebeaudeuf's method.[12]

The AlN layer is very thin, usually 1–2 nm. A reasonable premise is brought forward to simplify the solution. We suppose that the background electron concentration is zero in AlN material, so it is easy to learn that the electric field E_1 in AlN is a constant, which is obtained from the Poisson equation.

We set the potential in AlGaN as $V_2(x)$, and obtain

$$\left.\frac{{\rm d}V_2(x)}{{\rm d}x}\right|_{x=0} = -E_{\rm i2}, \tag{5}$$

from the Poisson equation:

$$\frac{{\rm d}^2V_2(x)}{{\rm d}x^2} = -\frac{qN_{\rm B}}{\varepsilon_2}, \tag{6}$$

where ε_2 is the dielectric constant of AlGaN, and $E_{\rm i2}$ is the electric field at $x = 0$ near the AlGaN side. Then an equation can be found from the integration of Eq. (6), and is given by

$$\frac{{\rm d}V_2(x)}{{\rm d}x} = -E_{\rm i2} - \frac{qN_{\rm B}x}{\varepsilon_2}. \tag{7}$$

We set the potential at $x = 0$ as the reference potential, that is $V_2(0) = 0$, so we can obtain the equation:

$$\int_0^{-d_2} \frac{\mathrm{d}V_2(x)}{\mathrm{d}x}\mathrm{d}x = V_2(-d_2) - V_2(0) = V_2(-d_2) = -V_2. \quad (8)$$

Note that the potential of conduction band at $x = -d_2$ is actually lower than that at $x = 0$, so

$$V_2 = |V_2(-d_2) - V_2(0)| = -V_2(-d_2),$$

where V_2 is an absolute value, marked in Fig. 2.

Another equation can be found by integrating Eq. (7), and is given by

$$\int_0^{-d_2} \frac{\mathrm{d}V_2(x)}{\mathrm{d}x}\mathrm{d}x = E_{\mathrm{i}2}d_2 - \frac{qd_2^2N_{\mathrm{B}}}{2\varepsilon_2}. \quad (9)$$

We will get

$$V_2 = \frac{qd_2^2N_{\mathrm{B}}}{2\varepsilon_2} - E_{\mathrm{i}2}d_2 \quad (10)$$

from Eqs. (8) and (9).

According to Gauss law, we obtain

$$\varepsilon_1E_1 = \varepsilon_2E_{\mathrm{i}2} = \varepsilon_3E_{\mathrm{i}3}, \quad (11)$$

where ε_1 is the dielectric constant in AlN.

The following relations can be found from Fig. 2:

$$\Delta E_{\mathrm{c}1} - V_1 = \phi_{\mathrm{M}} - V_{\mathrm{g}} + E_{\mathrm{F}}, \quad (12)$$

and

$$\Delta E_{\mathrm{c}2} + \Delta V - V_1 = V_2, \quad (13)$$

where

$$\Delta V = \varepsilon_1E_1 \quad (14)$$

is the voltage on AlN.

The sheet carrier concentration follows from Eqs. (4), (10)–(14):

$$n_{\mathrm{s}} = \frac{1/q}{\dfrac{d_1}{\varepsilon_1} + \dfrac{d_2}{\varepsilon_2}}\left(V_{\mathrm{g}} - \phi_{\mathrm{M}} - E_{\mathrm{F}} + \Delta E_{\mathrm{c}1} - \Delta E_{\mathrm{c}2} + \frac{qN_{\mathrm{B}}d_2^2}{2\varepsilon_2}\right) + N_{\mathrm{b}}W. \quad (15)$$

If the polarisation induced charge is taken into account,[14] Eq. (15) will be supplemented as

$$n_{\mathrm{s}} = \frac{1/q}{\dfrac{1}{C_1} + \dfrac{1}{C_2}}\left(V_{\mathrm{g}} - \phi_{\mathrm{M}} - E_{\mathrm{F}} + \Delta E_{\mathrm{c}1} - \Delta E_{\mathrm{c}2} + \frac{\sigma_{\mathrm{AlN}}}{C_1} + \frac{\sigma_{\mathrm{AlGaN}}}{C_2} + \frac{qN_{\mathrm{B}}d_2^2}{2\varepsilon_2}\right) + N_{\mathrm{b}}W, \quad (16)$$

with $C_1 = \varepsilon_1/d_1$ and $C_2 = \varepsilon_2/d_2$.

The capacitance per unit area of Schottky barrier can be deduced from Eq. (3), and is given by

$$C_{\mathrm{s}} = \frac{1}{\dfrac{1}{C_1} + \dfrac{1}{C_2}}\left(1 - \frac{\mathrm{d}E_{\mathrm{F}}}{\mathrm{d}V_{\mathrm{g}}} + \frac{\mathrm{d}\sigma_1}{C_1\mathrm{d}V_{\mathrm{g}}} + \frac{\mathrm{d}\sigma_2}{C_2\mathrm{d}V_{\mathrm{g}}}\right) + q\left(N_{\mathrm{b}}\frac{\mathrm{d}W}{\mathrm{d}V_{\mathrm{g}}} + W\frac{\mathrm{d}N_{\mathrm{b}}}{\mathrm{d}V_{\mathrm{g}}}\right) \quad (17)$$

with

$$qE_{\mathrm{F}} = qE_{\mathrm{F}0} - E_{\mathrm{c}} = \frac{kT}{q}\ln\left(\frac{n_0}{N_{\mathrm{c}}}\right),$$

where n_0 is the electron concentration at heterointerface, and N_{c} is the effective density of states in the GaN conduction band. If the polarisation induced charge has no relation with gate voltage, Eq. (17) reduces to

$$C_{\mathrm{s}} = \left(\frac{1}{C_1} + \frac{1}{C_2}\right)^{-1}\left(1 - \frac{kT}{q}\frac{\mathrm{d}\ln(n_0)}{\mathrm{d}V_{\mathrm{g}}}\right) + q\left(N_{\mathrm{b}}\frac{\mathrm{d}W}{\mathrm{d}V_{\mathrm{g}}} + W\frac{\mathrm{d}N_{\mathrm{b}}}{\mathrm{d}V_{\mathrm{g}}}\right). \quad (18)$$

3. Discussion

3.1. Analysis of the physical process for the reverse-biased CV profiling

According to the formation process of CV profiling, we define the curve nodes (A, B, C and D) in Fig. 3. The CV profiling is given by Atlas device simulation. The structure adopted in simulation is the same as the practical device, and some parameters are as follows: the thickness of AlGaN layer 13 nm (the remanent thickness after etching), AlN layer 1 nm, high mobility GaN layer 100 nm, high resistance GaN layer 1.5 μm. The detailed discussion on the process is combined with the expression Eq. (18).

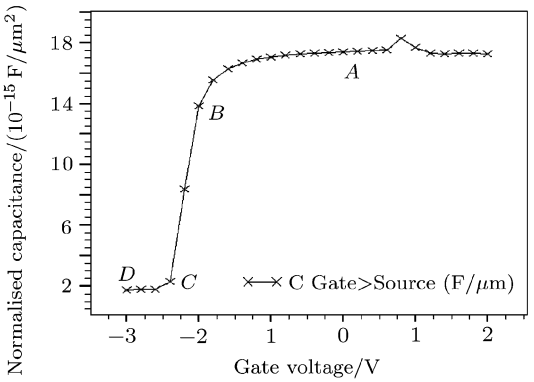


Fig. 3. Simulated CV profiling.

At gate zero-biased condition (point A), Fermi level at heterointerface is upon conduction (Fig. 2). The background donor impurity would not nearly ionise, that is $N_{\rm b}$= 0, because of the tremendous electron concentration at heterointerface, the change of n_0 under reverse-biased condition is very small. So Eq. (18) can be reduced to

$$C_{\rm s} = \left(\frac{1}{C_1} + \frac{1}{C_2}\right)^{-1}. \tag{19}$$

The capacitance reflects the thickness of the effective barrier. If the flat capacitance is too large, that is the effective barrier is too thin, we may think that the gate recess is over etched or the gate metal sinking happened without regard to the influence of trap. If we take the trap into consideration, the fringe capacitance may be responsible for the phenomenon.[5]

The minus voltage begins to apply on the gate, corresponding to section A to section B. The change of electron concentration at heterointerface can not be ignored now. So Eq. (18) can be reduced to

$$C_{\rm s} = \left(\frac{1}{C_1} + \frac{1}{C_2}\right)^{-1}\left(1 - \frac{kT}{q}\frac{{\rm d}\ln(n_0)}{{\rm d}V_{\rm g}}\right). \tag{20}$$

We can convert Eq. (20) to another useful expression: $C_{\rm s} = \varepsilon_{\rm e}/(d_1 + d_2 + \Delta d)$, where $\varepsilon_{\rm e}$ is the equivalent dielectric constant in barrier, $\Delta d = (\varepsilon_{\rm e}/q)\cdot({\rm d}E_{\rm F}/{\rm d}n_{\rm s})$ is the effective channel distance. The decrease of capacitance is due to the modulation of channel extending. According to depletion model, the depletion area is extending from heterointerface to GaN high mobility layer.

Point B is a key point. When it comes to point B, the electron concentration decreases to $\sim 10^{16}$ cm^{-3}, which is almost the same as the background level. The 2DEG is nearly depleted, and the depletion region is pushed to the bottom of the effective channel. At point B, 2DEG will ideally reduce to zero, so the capacitance will certainly reduce to zero. If we calculate the first-order differential of the capacitance, an infinite value will appear at point B. But due to the influence of the background concentration, the capacitance remains to nonzero value. At this moment, a maximum value will appear at point B for the first-order differential, and zero for the second-order differential. Obviously, point B is the inflexion of the ideal capacitance. We can also find that the threshold voltage is almost equal to the inflexion voltage.

The resident electron begins to ionise after point B in negative direction and the last two terms of Eq. (18) will react, that is

$$C_{\rm s} = \left(\frac{1}{C_1} + \frac{1}{C_2}\right)^{-1}\left(1 - \frac{kT}{q}\frac{{\rm d}\ln(n_0)}{{\rm d}V_{\rm g}}\right) + q\left(N_{\rm b}\frac{{\rm d}W}{{\rm d}V_{\rm g}} + W\frac{{\rm d}N_{\rm b}}{{\rm d}V_{\rm g}}\right). \tag{21}$$

Analysing Eq. (18) qualitatively, we can know that the smaller $V_{\rm g}$ is, the wider the depletion region is, that is ${\rm d}W/{\rm d}V_{\rm g} < 0$ and the smaller $V_{\rm g}$ is, the more the ionised background impurity is, that is ${\rm d}N_{\rm b}/{\rm d}V_{\rm g} < 0$. The equation indicates that the capacitance change rate has related to the material background concentration.

The depletion region is extending from the bottom of the effective channel to the high resistance layer, so the steep curve from B to C reflects the low electron concentration and the low leakage from the high mobility layer to the high resistance layer.

When it comes to point C, the electron concentration decreases to a lower level about 10^{15} cm^{-3}. The current is almost completely pinched off, and point C is actually pinch-off voltage. The depletion region is extending to the interface of high mobility layer and the high resistance layer or even in the high resistance layer.

After point C, the capacitance is very small, and the curve changes little. The edge of the depletion region will go deep into the high resistance layer. Because the free electron concentration is very low in the high resistance, the vertical width of depletion region will keep constant ideally, that is ${\rm d}W/{\rm d}V_{\rm g} = 0$. And the depletion region will extend horizontally.[15] The capacitance will be given by

$$C_{\rm s} = \left(\frac{1}{C_1} + \frac{1}{C_2}\right)^{-1}\left(1 - \frac{kT}{q}\frac{{\rm d}\ln(n_0)}{{\rm d}V_{\rm g}}\right) + qW\frac{{\rm d}N'_{\rm b}}{{\rm d}V_{\rm g}}, \tag{22}$$

where $N'_{\rm b}$ is the ionised background electron concentration in high resistance layer.

3.2. Analysis of the physical process for the forward-biased CV profiling

A few papers have suggested that the forward-biased CV profiling has some relation with the barrier material.[4] Under forward-biased conditions, we observe that there is rise or fall phenomenon of gate capacitance, presented in different papers and our measurements. In order to learn the ideal CV profiling under forward-biased condition, we carry on some

analogy from the conclusion of AlGaAs/GaAs HEMT, which will give us a basic judgment.

Early in 1985, Moloney *et al.*[16] and Norris *et al.*[9] had given a detailed decomposition chart of CV characteristics of AlGaAs/GaAs HEMT, which indicated each contribution of electron, hole, donor and acceptor to CV profiling. Refer to Fig. 2 in Ref. [16] and Fig. 1 in Ref. [9] for details. The risen phenomenon under forward-biased condition is observed on both figures said above, where the rising part is caused by donors in AlGaAs, while the falling part is caused by 2DEG. And the influence of free electron and acceptor on capacitance is little. AbdelRassoul *et al.*[17] had deduced the following gate capacitance expression of GaAs HEMT:

$$C = \frac{q^2 n_{\rm s}}{E(-d)\varepsilon_2 k_x} + \frac{qN_{\rm D}}{E(-d)} \times \left[\frac{1 - \dfrac{q(d-d_{\rm i})}{\varepsilon_2 k_x}}{1 + 2\exp\left(\dfrac{V'_{\rm G} - V'_{\rm c}}{V_{\rm T}}\right)} - \frac{1}{1 + 2\exp\left(\dfrac{V'_{\rm G} - V_{\rm d}}{V_{\rm T}}\right)} \right] + \frac{qN_{\rm c}}{E(-d)} \left[\frac{1}{0.27 + \exp\left(\dfrac{V_{\rm b} - V'_{\rm G}}{V_{\rm T}}\right)} - \frac{1 - \dfrac{q(d-d_{\rm i})}{\varepsilon_2 k_x}}{0.27 + \exp\left(\dfrac{V'_{\rm a} - V'_{\rm G}}{V_{\rm T}}\right)} \right].$$

Refer to Ref. [17] for detailed meanings of parameters. We can make out that the second term of the expression said above reflects the contribution of the donor, which is consistent with the decomposition chart.

The equivalent circuit diagram (Fig. 4) under forward bias is provided by Moloney *et al.*,[16] with C_1 and C_2 being equivalent barrier capacitance, G_1 and G_2 being the leakage conductance and R being the resistance of doped area. In theory, if $V_{\rm g} < 0$, the barrier layer is depleted, so it can be regarded as a flat capacitor; if $V_{\rm g} > 0$, and at the same time the barrier layer is heavily doped, the increase of $V_{\rm g}$ will lead to the increase of electron in the barrier layer which is supplied by donors, inducing the state of two capacitors (C_1 and C_2) in series as shown in Fig. 4. The 2DEG will go saturation with the increasing gate voltage, and finally the second capacitor (C_2) will cut no ice. The increased $V_{\rm g}$ will lead to increase electron in the barrier layer. Therefore the capacitance will rise because of a narrower distance of the capacitor C_1. If the barrier layer is not doped, the electron supplied by donors could not make up the increased potential, thus high density electron would not appear in the barrier layer, and certainly the capacitance will fall because of the saturated 2DEG.

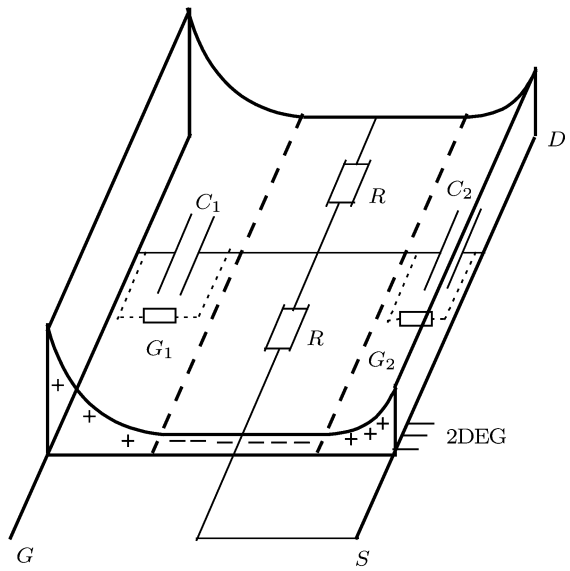


Fig. 4. Equivalent circuit diagram of GaAs/AlGaAs HEMT under forward-biased condition (from Ref. [16]).

However, CV profiling reflects the distribution of electron concentration, other than the distribution of doping. If the considerable electron from the tail of 2DEG distribution piles into the barrier layer, the capacitance will also slightly ascend.

Hence, the main reason of the rising capacitance under forward bias is the heavily doped barrier layer. At the same time, the considerable electron tails of 2DEG in the barrier also lead to a slight rise. On the contrary, if the barrier layer is not intentionally doped, and few electron enters the barrier layer, the gate capacitance under forward-biased application will fall ideally.

Guo *et al.*[14] had carried on the energy band simulation about AlGaN/GaN HEMT, including the structure with AlN interlayer, and obtained some useful data. Refer to Fig. 2 and Table 1 in Ref. [14] for details. As is shown in the table, the electron concentration in the barrier with AlN interlayer is

only 4.8% of the whole electron, but 13.3% without AlN interlayer. We may suppose that the unintentionally doped AlGaN/GaN HEMT gate capacitance is likely to rise slightly under forward-biased application. The rising part of the capacitance will lead to the small drop section beyond the peak towards M–S interface in electron distribution profiling. The speculation is agreed with the measurement reported by Jang *et al.*[18] However, the low concentration electron in the barrier with AlN interlayer can not produce the considerable capacitance when gate is forward-biased. Thus the capacitance will fall under forward-biased condition, which corresponds to the single-side peak electron distribution in electron distribution profiling. If a rising capacitance is observed obviously in this situation, it is likely that some uncertain factors bring in donor-like impurities in AlGaN or AlN layer, including the material grow process or the Inductive Couple Plasmas etch process.

We use LCR metre to measure CV characteristics of Schottky contacts. The structure of epilayers is given as Fig. 1. The diameter of Schottky contact is 150 μm. The measurement conditions of LCR metre are as follows: frequency (100 kHz, 1 MHz), level=0.1 V. The measured data is given by Fig. 5.

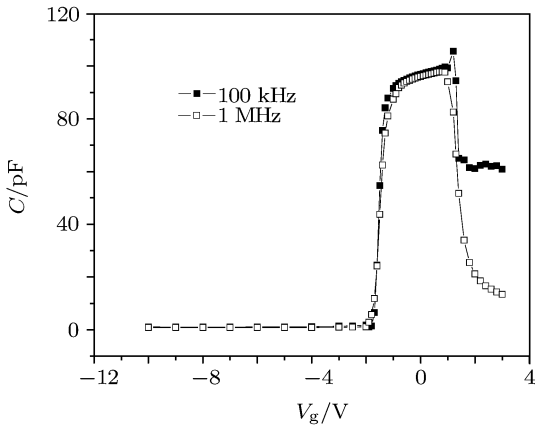


Fig. 5. The CV profiling with variable frequencies for Schottky contact.

We can obtain some informations from Fig. 5:

(i) Under forward bias, the gate capacitance will rise under low frequency measurement, and fall under high frequency measurement, which reflects that the electron in AlN or AlGaN layer is affected by the capture of traps, and the trapped electron has different responses to AC signal.

(ii) There is larger frequency dispersion on capacitance under forward bias than that under reverse bias, which reflects a higher trap density in the barrier than in GaN layer.

4. Conclusion

The gate CV relationship of GaN HEMT with AlN interlayer is calculated in this paper. The CV expression will help to analyse the physical process of CV profiling. The process can be separated into several sub-processes, which correspond to the evolution of depletion region edge in each epilayer under bias. Some material parameters related with each sub-process are given in the simplified expression. From the conclusion of reported researches on forward-biased CV profiling, we believe the gate capacitance of unintentionally doped GaN HEMT with AlN interlayer will fall under forward bias. If the capacitance rises obviously, it is likely that the donor-like impurities or traps occurred in the barrier layer. The experimental data agrees with our analysis.

Acknowledgement

The authors would like to thank Engineer Ouyang Sihua for compiling the CV measurement software and Li Yankui for maintaining the CV measurement system. Also we would like to thank the Institute of Semiconductors of CAS for supplying the epilayers of the device.

References

[1] Adikimenakis A, Aretouli K E, Iliopoulos E, Kostopoulos A, Tsagaraki K, Konstantinidis G and Georgakilas A 2009 *Microelectronic Engineering* **86** 1071

[2] Lisesivdin S B, Balkan N, Makarovsky O, Patane A, Yildiz A, Caliskan M D, Kasap M, Ozcelik S and Ozbay E 2009 *J. Appl. Phys.* **105** 6

[3] Qian F, Leach J H, Xie J Q, Ozgur U, Morkoc H, Zhou L and Smith D J 2009 *Proceedings of the SPIE — The International Society for Optical Engineering* **7216** 14

[4] Zhou Y G, Shen B, Liu J, Yu H Q, Zhou H M, Qian Y, Zhang R, Shi Y and Zheng Y D 2001 *Chin. J. Semiconductors* **22** 1420

[5] Liu W L, Chen Y L, Balandin A A and Wang K L 2006 *Journal of Nanoelectronics and Optoelectronics* **1** 258

[6] Hashizume T, Alekseev E, Pavlidis D, Boutros K S and Redwing J 2000 *J. Appl. Phys.* **88** 1983

[7] Wang R X, Xu S J, Shi S L, Beling C D, Fung S, Zhao D G, Yang H and Tao X M 2006 *Appl. Phys. Lett.* **89** 3

[8] Gorev N B, Kodzespirova I F, Kostylev S A, Kovalenko Y A and Prokhorov E F 1998 *5th Int. Conf. on Solid-State and Integrated Circuit Technology* Beijing, China, Oct. 21–23, 1998, p661

[9] Norris G B, Look D C, Kopp W, Klem J and Morkoc H 1985 *Appl. Phys. Lett.* **47** 423

[10] Kwangman P, Hong Bae K and Kae Dal K 1987 *IEEE Trans. Electron Devices* **34** 2422

[11] Zhou Y G, Shen B, Liu J, Zhou H M, Yu H Q, Zhang R, Shi Y and Zheng Y D 2001 *Acta Phys. Sin.* **50** 1774 (in Chinese)

[12] Delagebeaudeuf D and Linh N T 1982 *IEEE Trans. Electron Devices* **29** 955

[13] Anwar A F M and Faraclas E W 2006 *Solid-State Electronics* **50** 1041

[14] Guo L, Wang X, Wang C, Xiao H, Ran J, Luo W, Wang X, Wang B, Fang C and Hu G 2008 *Microelectronics Journal* **39** 777

[15] Kokorev M F and Maleev N A 1996 *Solid-State Electronics* **39** 297

[16] Moloney M J, Ponse F and Morkoc H 1985 *IEEE Trans. Electron Devices* **32** 1675

[17] AbdelRassoul R A, Yakout M A, AbdelFattah A I and Essa S G 2002 *Proceedings of the Nineteenth National Radio Science Conference* Alexandria, Egypt, May 19–21, 2002, p475

[18] Jang H W, Jeon C M, Kim K H, Kim J K, Bae S B, Lee J H, Choi J W and Lee J L 2002 *Appl. Phys. Lett.* **81** 1249